Quantum chemical determination of molecular geometries, interpretation of FT-IR, FT-Raman spectra and charge transfer properties for N-(2-cyanoethyl)-N-methylaniline

ARTICLE *in* SPECTROCHIMICA ACTA PART A MOLECULAR AND BIOMOLECULAR SPECTROSCOPY · JANUARY 2014

Impact Factor: 2.35 · DOI: 10.1016/j.saa.2013.12.084 · Source: PubMed

3 AUTHORS, INCLUDING:

Dr Vadivelu Balachandran
A.A.Government Arts College Musiri
155 PUBLICATIONS **672** CITATIONS

SEE PROFILE

Spectrochimica Acta Part A: Molecular and Biomolecular Spectroscopy 124 (2014) 1–11

Contents lists available at ScienceDirect

Spectrochimica Acta Part A: Molecular and Biomolecular Spectroscopy

journal homepage: www.elsevier.com/locate/saa

Quantum chemical determination of molecular geometries, interpretation of FT-IR, FT-Raman spectra and charge transfer properties for N-(2-cyanoethyl)-N-methylaniline

B. Revathi [a], A. Nataraj [b], V. Balachandran [a,*]

[a] Centre for Research, Department of Physics, Arignar Anna Government Arts College, Musiri, Tiruchirapalli 621211, India
[b] Department of Physics, SRM University, Chennai 600089, India

HIGHLIGHTS

- The FT-IR and FT-Raman spectra of N-(2-cyanoethyl)-N-methylaniline were analyzed.
- MEP surface provide information about donor and acceptor atoms in the molecule.
- Charge transfer characteristics were examined by HOMO-LUMO and NBO analysis.
- Thermodynamic properties were determined at different temperatures.
- UV-VIS spectral analyses have been researched by theoretical calculations.

GRAPHICAL ABSTRACT

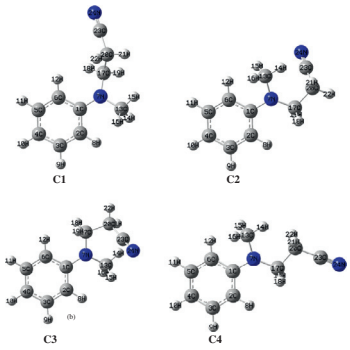

ARTICLE INFO

Article history:
Received 20 October 2013
Received in revised form 2 December 2013
Accepted 11 December 2013
Available online 4 January 2014

Keywords:
N-(2-cyanoethyl)-N-methylaniline
Molecular orbital studies
UV–VIS analysis
NBO
Electrostatic potential

ABSTRACT

FT-Raman and FT-IR spectra were recorded for N-(2-cyanoethyl)-N-methylaniline sample in solid state. The equilibrium geometries, harmonic vibrational frequencies, infrared and Raman scattering activities were computed using DFT method. Results obtained at this level of theory were used for a detailed interpretation of the infrared and Raman spectra, based on the potential energy distribution (PED) of the normal modes. Molecular parameters such as bond length, and bond angle were calculated with the same method. The intra-molecular charge transfer was calculated by means of natural bond orbital analysis (NBO). Hyperconjugative interaction energy was more during the π–π^* transition. Energy gap of the molecule was found using HOMO and LUMO calculation, hence the less band gap, which seems to be more stable. Atomic charges of various atoms of title molecule and other thermo-dynamical parameters were calculated using same levels of calculation. The correlation equations between heat capacity, entropy, Gibb's free energies changes with temperatures were fitted by quadratic formula. UV–VIS spectral analyses of title molecule have been researched by theoretical calculations. In order to understand electronic transitions of the compound, TD-DFT calculations on electronic absorption spectra in gas phase and solvent were performed. The calculated frontier orbital energies, absorption wavelengths (λ), oscillator strengths (f) and excitation energies (E) for gas phase in different solvent are also illustrated.

* Corresponding author. Tel.: +91 431 2591338; fax: +91 432 6262630.
E-mail address: brsbala@rediffmail.com (V. Balachandran).

1386-1425/$ - see front matter
http://dx.doi.org/10.1016/j.saa.2013.12.084

Introduction

Nitrile is an organic compound containing cyano group (—C≡N, containing trivalent nitrogen) which is attached to one carbon atom with the general formula RC≡N. Their names are corresponding to carboxylic acids by changing '-ic acid' to the suffix, '-onitrile' which denotes only the ≡N atom excluding the carbon atom attached to it, or the suffix, '-carbonitrile' where the carbon atom in the —CN is included, whichever preserves a single letter O. Examples are acetonitrile from acetic acid and benzonitrile from benzoic acid. The prefix, 'cyano-' is used as an alternative naming system to indicate the presence of a nitrile group in a molecule for the compounds of salts and organic derivatives from the isomer, $HN^{+}{\equiv}C$. Sodium cyanide, NaCN; potassium cyanide, KCN; calcium cyanide, $Ca(CN)_2$; and hydrocyanic (or prussic) acid, HCN are examples. Chemically, the simple inorganic cyanides resemble chlorides in many ways. Organic nitrile act as solvents and are reacted further for various application including; extraction solvent for fatty acids, oils and unsaturated hydrocarbons. Solvent for spinning and casting and extractive distillation based on its selective miscibility with organic compounds. It is parent compound for organic synthesis. It is used as a solvent or chemical intermediate in biochemistry, also used solvent for perfumes and pharmaceuticals [1].

In the present work, harmonic-vibrational frequencies calculated for stable conformer of N-(2-cyanoethyl)-N-methylaniline [hereafter referred as CMA] using B3LYP/6-311++G(d,p), and B3LYP/6-311G methods. The calculated spectrum of this conformer is compared to that of experimentally observed FT-IR and FT-Raman spectra. The redistribution of electron density (ED) in various bonding and antibonding orbitals and $E(2)$ energies have been calculated by natural bond orbital analysis by DFT/B3LYP/6-311++G(d,p) method to give clear evidence of stabilization originating from the hyper conjugation of various intramolecular interactions. The HOMO and LUMO energies have been calculated for different solvent and kinetic stability were analyzed. These are confirming the charge transfer within the molecule and also molecular electrostatic potential (MESP) contour map shows the various electrophilic and nucleophilic regions of the title molecule. However, molecular hyperpolarizability is also calculated by DFT/B3LYP/6-311++G(d,p), and DFT/B3LYP/6-311G methods. Finally, the correlations between thermodynamic parameters with various temperatures are reported.

Experimental and computational details

The FT-IR of the N-(2-cyanoethyl)-N-methylaniline was measured in the Bruker IFS 66V spectrometer in the range 4000–400 cm^{-1}. The FT-Raman spectrum of the N-(2-cyanoethyl)-N-methylaniline was also recorded in FT-Raman BRUKER RFS 100/S instrument equipped with Nd:YAG laser source operating at 1064 nm wavelength and 150 mW power. The spectrum is recorded in the range 3500–100 cm^{-1}. The spectral resolution is ±2 cm^{-1}. The initial geometry of CMA molecule optimized using the DFT with B3LYP using 6-311++G(d,p) and 6-311G levels of GAUSSIAN 09W [2]. The optimized molecular geometries, vibrational frequencies, IR, Raman intensities, force constants and other electronic properties were calculated.

Results and discussion

The molecular structure along with numbering of atoms is obtained from Gaussian 09W program and is as shown in Fig. 1 (C1). The global minimum energy obtained by DFT/B3LYP method structure optimization using 6-311++G(d,p) and 6-311G basis sets for the CMA molecule as −497.879372607, −497.725907833 hartrees, respectively. The energies of the molecule are presented in Table 1. This most optimized structure utilized for the further quantum chemical calculations.

Vibrational spectral analysis

The N-(2-cyanoethyl)-N-methylaniline molecule belongs to C_s point group symmetry and the total 66 normal modes are distributed into two types of vibrations namely A′ (in-plane) and A″ (out-plane). The irreducible representation for the C_s symmetry is given by $\Gamma_{Vib} = 45A' + 21A''$. All the vibrations are active in both IR and Raman spectra. Vibrational spectral assignments have been carried out on the recorded FT-IR and FT-Raman spectra based on the theoretically predicted wavenumbers by B3LYP with 6-311++G(d,p), 6-311G large basis sets along with their PED values and are presented in Table 2. The calculated wavenumbers all are positive values and confirm the optimized structure of the C1 conformer is the most stable. The calculated frequencies from DFT method are usually larger than the equivalent experimental values and contain known systematic errors due to the neglect of anharmonicity and electron correlation [3–6]. Hence, most of the calculated frequencies are well matches with the experimental values. Comparative IR and Raman spectrographs between the observed wavenumbers from the recorded spectra and the theoretical wavenumbers by B3LYP method have been plotted using pure Laurentian band shape with a band width of FWHM of 2 cm^{-1} are shown in Figs. 2 and 3, respectively.

Carbon–carbon vibrations

The ring carbon–carbon stretching vibrations occur in the region 1430–1625 cm^{-1}. In general, the bands are of variable intensity and are observed at 1625–1590, 1575–1590, 1470–1540, 1430–1465 and 1280–1380 cm^{-1} from the frequency ranges given by Varsanyi [7] for the five bands in the region. In the present work, the frequencies observed in FT-IR spectrum at 1599 and 1501 cm^{-1} have been assigned to C—C stretching vibrations. The corresponding vibration appears in the FT-Raman spectrum at 1605 cm^{-1}. The theoretically computed values of CMA at 1615, 1557, 1550, 1542, 1533 and 1509 cm^{-1} by B3LYP/6-311G and the bands at 1615, 1564, 1545, 1536, 1499 and 1496 cm^{-1} by B3LYP/6-311G++(d,p) method. These are shows excellent agreement with experimental data. The substituted νC—C band observed at 1655 cm^{-1} in FT-IR is nearly agreement with the experimental values. The in-plane deformation vibration is at higher frequencies than the out-of-plane vibrations. These are observed at 689, 611 cm^{-1} (IR), and 753, 717, 621 cm^{-1} (Raman) are assigned to CCC deformation of phenyl ring. There is no bands observed for the out-plane vibration due to their experimental spectral limits. The theoretically computed values at 736, 717, 650 cm^{-1} and 733, 699, 632 cm^{-1} by B3LYP/6-311G, B3LYP/6-311++G(d,p) methods, respectively, gives excellent agreement with experimental data. The in-plane C—C12, C17—C predicted medium to very strong bands observed at 811, 767 cm^{-1} in FT-IR and medium peak at 813 cm^{-1} in FT-Raman spectrum.

Aromatic CH vibrations

In the present study, the five hydrogen atoms (H8, H9, H10, H11 and H12), which are attached to the benzene ring of CMA give rise to five C—H stretching modes (66–62), five C—H in-plane bending (39–36, 28) and five C—H out-of-plane bending (27, 26, 24–22) modes are calculated. Usually the heteroaromatic organic molecule shows the presence of the C—H stretching vibrations in the

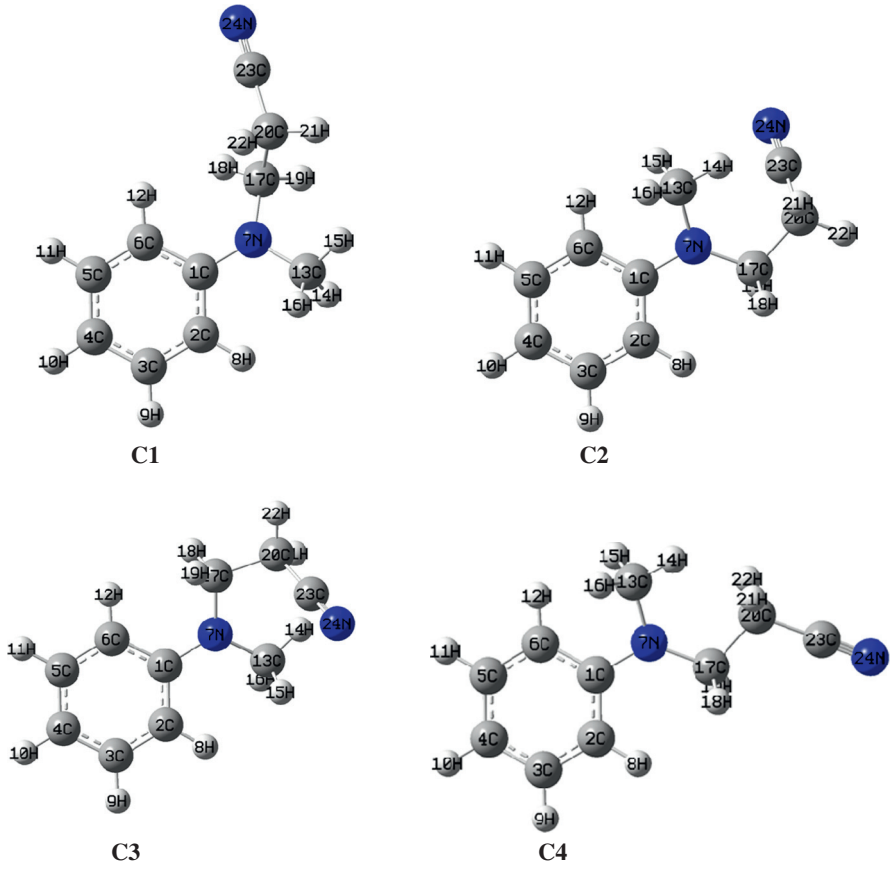

Fig. 1. Possible conformers of N-(2-cyanoethyl)-N-methylaniline.

wavenumber region 3000–3100 cm^{-1} and it is the characteristic region for the identification of C—H stretching vibrations [8]. For CMA molecule, the aromatic C—H stretching modes are assigned to 3157 cm^{-1} in FT-IR. The calculated theoretical wavenumbers at B3LYP/6-311++G(d,p) method for C—H stretching modes are comes under the reported region of wavenumbers and potential energy distribution (PED) results showed that, these modes are very pure. For toluic acid (TA), the bands at 3080, 3030 and 3020 cm^{-1} in FT-IR and 3050, 3030 cm^{-1} in FT-Raman have been assigned as C—H stretching modes by Babuet et al. [9]. In our previous work, we have assigned 3095, 3060 cm^{-1} in FT-IR and 3054 cm^{-1}in FT-Raman bands as C—H stretching modes of 5-nitrosalicylic acid (also known as 2-hydroxy-5-nitro benzoicacid) [10]. In aromatic compounds, the C—H in-plane and out-of-plane bending vibrations appear in the range 1000–1300 cm^{-1} and 750–1000 cm^{-1} [11–13], respectively. Hence, the C—H in-plane bending modes of the CMA molecule are attributed to 1289, 1266 and 1233 cm^{-1} in FT-IR and 1295 cm^{-1} in FT-Raman. The percentage of PED depicted in the last column of Table 2 shows that, CH_2 in-plane bending and C—C stretching vibrations are interacting considerably with C—H in-plane bending mode. The very strong to medium bands observed at 994, 873 cm^{-1} in FT-Raman and at 867 cm^{-1} in FT-IR are ascribed to C—H out-of plane bending modes of the title molecule. Thus the theoretical wavenumbers of C—H out-of plane bending modes depicted in Table 2 are found to be in agreement with the experimental data of CMA as well as the similar kind of molecules [11,12].

Methylene group vibrations

For the assignments of CH_2 group frequencies, basically six fundamentals can be associated to each CH_2 group namely, CH_2 sym, symmetric stretch, CH_2 asym, asymmetric stretch, CH_2 scis, scissoring and CH_2 rock, rocking modes which belong to polarized in-plane vibrations of species. In addition to that CH_2 wag, wagging and CH_2 twist, twisting modes of CH_2 group would be expected to be depolarized for out-of-plane bending vibrations. The C—H stretching vibration of the methylene group is at lower frequencies than those of the aromatic C—H ring stretching. The asymmetric CH_2 stretching vibration generally observed in the region 3000–2900 cm^{-1}, while the CH_2 symmetric stretch will appear between 2900 and 2800 cm^{-1} [14,15]. The CH_2 asymmetric and symmetric stretching vibrations are observed in FT-IR and FT-Raman spectrum as a weak intensity bands as seen in Table 2 for our title molecule. The band at 3044 and 2927, 2822 cm^{-1} in FT-IR are assigned to CH_2 asymmetric and symmetric stretching vibration, respectively. However, in view of our results, the assignment of CH_2 asymmetric stretching band, should be corrected (The FT-IR band at 3044 cm^{-1} was assigned to a asymmetric stretching of CH_2). The theoretically computed anharmonic wavenumbers by B3LYP/6-311+G(d,p) method at 3057, 3040, 3024, and 2664 cm^{-1} (mode nos. 58–55) are assigned to CH_2 asymmetric and symmetric stretching vibrations for CH_2 unit as shown in Table 2. The PED corresponding to both (asymmetric and symmetric) type of vibrations are combined with ϑC—H as it is evident from Table 2. In the present assignment the CH_2 bending modes follow, in decreasing wavenumber, the general order CH_2 deformation > CH_2 wagging > CH_2 rock > CH_2 twist. Since the bending modes involving hydrogen atom attached to the central carbon falls into the 1450–875 cm^{-1} range, there is extensive vibrational coupling of these modes with CH_2 deformations particularly with the CH_2 twist. It is notable that both CH_2 scissoring and CH_2 rocking modes were sensitive to the molecular confirmation. For cyclohexane, the CH_2 scissoring mode has been assigned to the medium intensity IR

Table 1
Total energy of different conformations are N-(2-cyanoethyl)-N-methylaniline calculated at the DFT (B3LYP)/6-311++G(d,p), and 6-311G levels of theory.

Conformers	Total energies (hartrees) 6-311++G(d,p)	Energy different With respect to (hartrees)	Total energies (hartrees) 6-311G	Energy different With respect to C1 (hartrees)
C1[a]	−497.879372607	0.00	−497.725907833	0.00
C2	−497.871323525	0.00805	−497.717921197	0.00799
C3	−497.760336559	0.11903	−497.600106659	0.1258
C4	−497.877024213	0.00234	−497.723282145	0.00262

[a] Global minimum energy (stable conformer).

band at about 1450 cm^{-1} was assigned to CH_2 scissoring mode [16]. In our title molecule the anharmonic frequency computed by B3LYP/6-311++G(d,p) method at 1468, and 1463 cm^{-1} (mode nos. 46,45) is assigned to CH_2 scissoring. The observed band at 1463 cm^{-1} in FT-Raman 1445 cm^{-1} in IR are well matches with the calculated B3LYP/6-311++G(d,p) method. The calculated PED corresponding to this mode show that this mode is a pure mode nearly 90%. The CH_2 wagging vibrations computed by B3LYP/6-311+G(d,p) method at 1367, 1350 cm^{-1} (mode nos. 42, 41). The PED corresponding to these modes are only 34%. The CH_2 twisting vibrations are observed as a weak band in FT-Raman spectrum at 450 cm^{-1}. The PED analysis identifies the CH_2 twisting vibration combined with C—H out-plane bending and C—C out-plane vibrations as evident from Table 2. The PED corresponding to this mode is 37%. The computed anharmonic wavenumber for this mode are at 463, 419 cm^{-1} (mode nos. 13, 12). The CH_2 rocking vibration computed by B3LYP method shows good agreement with experimental observations, the PED corresponds to the CH_2 rocking vibration is ∼35% (mode nos. 35, 34).

CH_3 group vibrations

In N-(2-cyanoethyl)-N-methylaniline, two CH_3 asymmetric stretching vibrations are assigned to bands at 3094, 3089 cm^{-1}. The band at 3075 cm^{-1} is assigned to CH_3 symmetric stretching vibration. These bands have been observed in similar systems [17,18]. All the three bands are raised in frequency of about 20 cm^{-1}, due to the presence of strong electronegative substituents [11]. The CH_3 deformation vibrations are expected in the region 1460–1436 cm^{-1} [17,18]. In N-(2-cyanoethyl)-N-methylaniline, two CH_3 asymmetric deformation vibrations are assigned to band at 1422 cm^{-1} in FT-IR and 1439 cm^{-1} in FT-Raman the computed band at 1416, 1396 cm^{-1} (B3LYP/6-311++G(d,p)). A strong band 1322 cm^{-1} is assigned to CH_3 symmetric deformation vibration. Red shift in CH_3 symmetric and asymmetric deformations observed, and is probably due to the presence of strong electronegative substituent. The CH_3 perpendicular rocking vibration is assigned to a strong band at 1122 cm^{-1} and the CH_3 parallel rocking vibration is assigned to a weak Raman band at 967 cm^{-1} and is in the expected range [19]. Torsional vibration for CH_3 is assigned to weak computed band at 138 cm^{-1}.

CN vibrations

The bond between C1, C13, C17 atoms of the benzene ring and N7 atom of the substituents gives rise to nine vibrational modes; C—N stretching (CN), C—N in-plane bending (βC—N) and C—N out-of plane bending (γC—N) vibrations. Generally, the identification of C—N bands in both the FT-IR and FT-Raman spectra are rather a difficult task, since these bands are highly mixed with other vibrations. In the present study, the strong intensity band at 1044 cm^{-1} in FT-IR and 1042 cm^{-1} in FT-Raman is assigned to C—N stretching mode of CMA. In previous, we have reported C—N stretching at 928 cm^{-1} in FT-Raman for 5-nitrosalicylic acid [10]. The peaks corresponding to C—N in-plane vibrations are 394, 374, 323 cm^{-1} (mode nos. 11–9) in FT-Raman. The out-of-plane bending modes of the investigated compound are not observed in both FT-IR and FT-Raman spectrum. Hence with the aid of PED results, the calculated values of 387, 374, 338, and 287, 246, 210 cm^{-1} are assigned to C—N in-plane and out-of plane bending modes, respectively at B3LYP/6-311++G(d,p).

Nitrile group modes

The C≡N stretching frequency is highly localized within the C≡N group. The characteristics frequency of C≡N stretching vibration of benzonitrile [20–22] falls in the region 2220–2240 cm^{-1} spectral range and it appears with strong Raman intensity whereas its IR intensity varies from medium-strong to strong depending upon the substituent(s). In benzonitrile this band has been identified at 2230 cm^{-1} and IR intensity have been correlated to the Hammett-type substitution parameters both experimentally and theoretically [23,24]. Electron-withdrawing groups, as —F, —NO_2, —OH, or —CF_3, decrease the IR band intensity and increase the frequency to the higher limit of the characteristic spectral region, whereas electron-donating groups, such as —NH_2, or —CH_3 increase the IR intensity and decrease the frequency [24]. Successive substitution of electron-withdrawing or donating groups can also shift the C≡N stretching frequency beyond the characteristic frequency region mentioned above. e.g. in 2,3,5,6-tetra-fluoro-4-cyano-benzonitrile [25], it is at 2353 cm^{-1}. The Raman intensity of the C≡N stretching is enhanced by the conjugation of the aromatic ring. Nevertheless, the aromatic ring stretching and deformation modes often exhibit stronger Raman intensities than the C≡N stretching vibration.

In the present case this characteristic frequency is observed at 2244 cm^{-1} in IR spectrum, and the band at 2262 cm^{-1} in Raman spectrum, these are observed very strong intense peak in both the FTIR and FT-Raman spectra. Due to the substituent effect on the molecule, intensity, and frequency are different in the spectra. The calculated band at 2261, 2283 cm^{-1} by B3LYP/6-311++G(d,p) as well as B3LYP/6-311G methods are agreement with the experimental spectra. In previous work we have reported C≡N stretching mode is 2228 cm^{-1} in FT-IR and the same peak 2227 cm^{-1} in FT-Raman spectrum of p-acetylbenzonitrile molecule [26]. The in-plane and out-of-plane bending vibrations of the nitrile group are linear bending type. These linear in-plane and out-of-plane bending vibrations have been assigned at the magnitude of 566 (IR), 578 (Raman) cm^{-1}, respectively. This in-plane mode is observed medium peak at IR spectrum, and weak band at Raman. The C≡N in-plane bending vibration strongly coupled with C—H out-plane bending and the ring angle bending vibrations. The C≡N out-of-plane bending vibration is lightly coupled with all the three C—H out-plane bending vibrations and strongly coupled with the ring out-plane mode.

Table 2
Comparison of the experimental (FT-IR and FT-Raman) wavenumbers (cm^{-1}) and theoretical wavenumbers (cm^{-1}) of N-(2-cyanoethyl)-N-methylaniline calculated by B3LYP/6-311++G(d,p), and B3LYP/6-311G methods.

Mode no.	Symmetry species	Experimental		DFT/6-311G			DFT/6-311++G(d,p)			Vibrational assignments PED[a] ⩾ 10%
		FT-IR	FT-Raman	Wavenumber (cm^{-1})	I_{IR}	I_{Raman}	Wavenumber (cm^{-1})	I_{IR}	I_{Raman}	
1	A″			36	3.0505	99.76	22	2.4796	99.9	γCCC (47), τCH$_3$ (18)
2	A″			43	4.0759	41.952	33	1.0403	22.91	γCCC (51), γCH$_2$ (18)
3	A″			80	1.8253	3.854	67	5.7822	2.0356	γCCC (68), τCH$_3$ (14)
4	A″			131	4.4658	4.602	138	1.5637	1.7949	τCH$_3$ (71)
5	A″		171vw	182	1.4294	1.748	188	5.7616	0.2768	γC≡N(79), γCCC (11)
6	A″			216	0.4396	1.081	210	2.2038	0.7217	γCN (41), γCCC (28)
7	A″			239	1.8751	0.9621	246	0.8424	0.1471	γCN (27), γCCC (15), γCH$_3$ (11)
8	A″			301	0.9230	0.467	287	0.9340	0.1840	γCN (30), γCH$_3$ (18), τCH$_2$ (13)
9	A′		323vw	334	8.4719	1.6305	338	6.9046	0.0464	βCN (38), γCCC (19), τCH$_3$ (15)
10	A′		371vw	371	0.2874	0.7401	374	0.1935	0.2095	βCN (38), γCCC (18), γCH (14)
11	A′		394vw	385	0.5241	0.8172	387	0.3763	0.2504	βCN (42), γCCC (21), τCH$_2$ (12)
12	A″			432	0.4364	0.0543	419	0.7436	0.0103	τCH$_2$ (49), γCCC (22), γCH$_3$ (13)
13	A″		459vw	472	1.6911	0.4684	463	1.6679	0.1401	τCH$_2$ (37), γCCC (17), γCH (12)
14	A″	512ms		536	5.1356	0.2388	524	12.2842	0.03092	γC17C (47), γCCC (16)
15	A″			540	7.9824	0.0881	529	4.6321	0.01135	γCC12 (43), γCH (35)
16	A′	566ms	578vw	580	11.5675	0.1375	584	4.7444	0.1559	βC≡N (48), γCCC (20), γCH (12)
17	A′	611vw	621w	650	0.4507	0.5697	632	0.2090	0.1623	βCCC (45), βCH (23)
18	A′	689vs	717ms	717	32.9343	0.0758	699	38.4850	0.0035	βCCC (65), βCH (24)
19	A′		753ms	736	2.8807	1.4385	733	1.5009	0.4496	βCCC (53), βCH (30)
20	A′	767vs		784	69.1527	0.0247	760	46.6306	0.067	βC17C (43), βCH (39)
21	A′	811ms	813ms	824	2.8560	0.4239	811	3.2074	0.2172	βCC12 (58), γCH (12)
22	A″			847	0.6058	0.1809	817	0.8722	0.0409	γCH(55), γCCC (25)
23	A″	867s	873ms	890	14.7280	0.4718	873	4.0299	0.28118	γCH(42), γCCC (20)
24	A″			914	8.3512	0.0876	881	3.5057	0.0523	γCH(57), βCCC (11)
25	A″	967vs	958w	988	0.1715	0.1548	963	0.0794	0.00212	γCH$_3$opr (58), γCH (24)
26	A″	988vs	994vs	994	15.8615	1.375	986	0.5754	0.0268	γCH (78)
27	A″			1013	0.4671	0.052	996	33.6716	0.2743	γCH (55), νCCC (25)
28	A′			1017	21.1519	0.6113	1001	3.0433	0.0946	βCH (49), νCCC (21)
29	A′			1027	9.4130	1.5473	1006	10.0131	0.8279	νCN (42), γCH (17)
30	A′	1044vs	1042vs	1056	7.8629	1.0775	1049	14.4193	0.427	νCN (37), βCH (20)
31	A′			1065	23.9497	0.3796	1055	14.8311	0.4598	νCN (35), βCH (15)
32	A′			1119	0.7337	0.0464	1112	2.2660	0.0145	νCC12 (54), νCN (17)
33	A′	1122vs	1139w	1147	16.5247	0.3845	1133	15.7248	0.0518	βCH$_3$ipr (64), βCH (21)
34	A″	1155ms	1163ms	1155	23.8053	0.2457	1194	23.7843	0.0839	δCH$_2$asb (48), βCH (17)νCC (14)
35	A″	1199vs	1199ms	1212	1.0552	0.2597	1199	0.7570	0.09174	δCH$_2$asb (35), βCH (23)νCC (11)
36	A′	1233s		1239	35.8000	0.1048	1233	7.8163	0.0276	βCH (52), βCC (24), δCH$_2$asb (23)
37	A′			1248	17.4731	0.1612	1240	34.4476	0.1579	βCH (49), νCC (16), CH$_2$ twist (13)
38	A′	1266s		1274	95.6093	0.1946	1265	78.0763	0.0749	βCH (54), νCC (24)
39	A′	1289ms	1295vw	1290	24.1820	0.3587	1269	18.4010	0.0549	βCH (61), νCC (16)
40	A′	1322s		1341	1.6930	0.207	1335	0.6410	0.0768	βCH$_3$sb (57), βCH (17), νCN (18)
41	A″	1356vs		1373	4.6840	0.4121	1350	24.4536	0.1874	ωCH$_2$ (41), βCH$_3$sb (35), νCC (13)
42	A″		1379ms	1398	6.8516	0.1058	1367	2.9925	0.02217	ωCH$_2$ (34), βCH (21), νCC(13)
43	A′			1413	73.4644	1.0722	1396	13.4775	0.072	βCH$_3$asb (75), β CH (22)
44	A′	1422ms	1439vw	1424	12.3607	0.3151	1411	80.6889	0.248	βCH$_3$asb (62), βCH (11)
45	A′	1445ms	1451vw	1497	5.9655	0.4668	1463	9.3652	0.0927	ρCH$_2$ (85)
46	A′		1463vw	1502	0.6576	0.0568	1468	9.1938	0.1374	ρCH$_2$ (92)
47	A′	1501vs		1509	10.9858	0.3233	1496	0.0749	0.0324	νCCC (68), βCH$_3$asb (24)
48	A′			1533	26.4323	0.5342	1499	16.5689	0.027	νCCC (64), βCH (22)
49	A′			1542	1.1014	0.8621	1536	9.1975	0.0819	νCCC (57), ρCH$_2$ (41)
50	A′			1550	55.8512	0.0612	1545	0.9391	0.0306	νCCC (52), βCH (40)
51	A′			1557	62.0329	0.4911	1564	138.4477	0.02506	νCCC (69), βCH (14)
52	A′	1599vs	1605vs	1615	10.6469	0.1812	1615	10.6721	0.07485	νCCC (66), βCH (26)
53	A′	1655w		1644	109.8142	2.013	1642	116.1048	0.7604	νC17C (64), βCH (18)
54	A′	2244vs	2262vs	2283	8.9758	0.935	2261	9.6997	0.4262	νC≡N (87), νCCC (12)
55	A′	2822ms	2833w	2880	87.9045	1.296	2829	71.9043	0.5008	νCH$_2$ss (88), βCH (12)
56	A′	2927ms	2952ms	2976	79.8489	1.3811	3024	41.7709	0.2857	νCH$_2$ss (63), βCH (15)
57	A′	3044ms		3025	24.5413	1.5709	3040	25.8454	0.7128	νCH$_2$ass (77), βCH (22)

(*continued on next page*)

Table 2 (*continued*)

Mode no.	Symmetry species	Experimental		DFT/6-311G			DFT/6-311++G(d,p)			Vibrational assignments PED[a] ⩾ 10%
		FT-IR	FT-Raman	Wavenumber (cm^{-1})	I_{IR}	I_{Raman}	Wavenumber (cm^{-1})	I_{IR}	I_{Raman}	
58	A′			3061	6.9643	0.5723	3057	37.6423	0.3563	νCH_2ass (68), βCH (32)
59	A′	3066ms		3063	38.4226	0.7056	3075	3.3954	0.1963	νCH_3ss (71), βCH (16)
60	A′	3088vw		3090	24.3582	0.3302	3089	20.8467	0.1735	νCH_3ass (58), βCH (27)
61	A′			3092	14.1498	0.2812	3094	7.8386	0.0574	νCH_3ass (65), βCH (25)
62	A′			3095	5.4229	0.3649	3097	4.7171	0.1101	νCH (95)
63	A′		3100ms	3101	17.9410	0.7843	3099	10.0477	0.258	νCH (98)
64	A′	3177vw		3103	46.7168	0.6281	3106	29.1190	0.1642	νCH (97)
65	A′			3107	26.2915	0.0687	3110	13.8456	0.3747	νCH (98)
66	A′			3122	1.3551	1.6391	3115	6.2777	0.2895	νCH (98)

ν; Stretching, β; in-plane bending, γ; out-of-plane bending, τ; torsion, s; strong, vs; very strong, ms; medium strong, w; weak, vw; very weak, A′ ; in-plane of vibrations, A″ ; out-of-plane vibrations, ρ ; scissoring, ω; wagging, δ; rocking.

[a] Potential energy distribution.

NBO analysis

Natural bond analysis gives the accurate possible natural Lewis structure picture of φ because all orbital mathematically chosen to include the highest possible percentage of the electron density. Interaction between both filled and virtual orbital spices information correctly explained by the NBO analysis, it could enhance the analysis of intra- and intermolecular interactions. The second order Fock matrix was carried out to evaluate donor (i) acceptor (j) i.e. donor level bonds to acceptor level bonds interaction in the NBO analysis [27]. The result of interaction is a loss of occupancy from the concentrations of electron NBO of the idealized Lewis structure into an empty non-Lewise orbital. For each donor (i) and acceptor (j), the stabilization energy $E(2)$ associates with the delocalization $i \rightarrow j$ is estimated as,

$$E_2 = \Delta E_{ij} = q_i \frac{F(i,j)^2}{\varepsilon_j - \varepsilon_i}$$

where q_i is the donor orbital occupancy, are ε_j and ε_i diagonal elements and $F(i,j)$ is the off diagonal NBO Fock matrix element. Natural bond orbital analysis is used for investigating charge transfer or conjugative interaction in the molecular system. Some electron donor orbital, acceptor orbital and the interacting stabilization energy resulted from the second-order micro-disturbance theory are reported [28,29]. The larger $E(2)$, value the more intensive is the interaction between electron donor and acceptor, i.e. the more donation tendency from electron donors to electron acceptors and the greater the extent of conjugation of the whole system [30]. Delocalization of electron density between occupied Lewis-type (bond or lone pair) NBO orbitals and formally unoccupied (antibond or Rydgberg) non-Lewis NBO orbitals correspond to a stabilization donor–acceptor interaction. NBO analysis has been performed on the C1 conformer of CMA molecule at the DFT/B3LYP/6-311++G(d,p) level in order to elucidate the intramolecular, rehybridization and delocalization of electron density within the molecule.

The intramolecular interaction is formed by the orbital overlap between σ(C1—C2), σ(C5—C6) and σ*(C1—C6), σ*(C1—N7) bond orbital, which results intramolecular charge transfer causing stabilization of the system. The most important interactions in the title molecule having lone pair N7(1) with that of antibonding π*(C1—C6) and the lone pair N24(1) with that of antibonding σ*(C20—C23) results the stabilization of 30.29 kJ mol^{-1} and 9.81 kJ mol^{-1}, respectively, which donates larger delocalization. The maximum energy transfer occurs from LPN7(1) and LPN24(1) to π*(C1—C6) and σ*(C20—C23) as shown in Table 3. The ED in N7(1) and N23(1) lone pairs are moderates increased the electron density of σ*(C20—C22) and π*(C1—C2) are of 0.02124 e and 0.02145 e, respectively, which yields to weakening the bond and its elongation (0.145 and 0.075 Å) from the ring carbon atoms of the title molecule.

Atomic charges and HOMO, LUMO analysis

The calculation of atomic charges plays a key role in the application of quantum mechanical calculation to describe the electronic characteristics of molecular systems [31]. The calculated Mulliken atomic charges at DFT/B3LYP/6-311++G(d,p) are presented in Table 4. Significant change in the atomic charges of carbon atoms C1 and C6 were found in the molecule arises upon the electronic effects by the hydrogen atoms attached with them. Considering the charges of title molecule, the atom C6 having more positive charges (0.291668 eV), indicates the high electron withdrawing nature, as it is linked between the neighboring C1 and C5 atoms through double bond. Likewise high negative values were observed in methylene and methyl groups carbon atoms C17 (−0.565487 eV) and C13 (−0.419933 eV). The variations in the atomic charges of remaining atoms with the natural charges are presented in Table 4.

We obtained a plot of the frontier molecular orbital of the title molecule (HOMO and LUMO) to analyze the main atomic contributions for theses orbitals. The importance of observing these plots was to determine the chemical reactivity of title molecule. The HOMO (highest occupied molecular orbital) energy characterizes the ability of electron giving; LUMO (lowest unoccupied molecular orbital) energy characterizes the ability of electron accepting [32]. The energy gap between HOMO and LUMO characterizes the molecular chemical stability and it is a critical parameter in determining molecular electrical transport properties because it is a measure of electron conductivity. Relatively large LUMO–HOMO energy gap of the studied molecule indicates that it can be considered as kinetically stable. In addition, energy of the HOMO is directly related to the ionization potential, while energy of the LUMO is directly related to the electron affinity. The energy gaps are largely responsible for the chemical and spectroscopic properties of the molecules [33]. The features of the HOMO and LUMO also calculated by TD-DFT/B3LYP/6-311++G(d,p) in water, ethanol, and methanol in gaseous phase. The TD-DFT calculation in water, ethanol, and methanol, the energy band gap (ΔE) of the molecule is about 0.18593, 0.18124 and 0.18119 a.u. According to that the energy gap (ΔE = 0.18593 a.u.) calculated at water is more than the other. This value indicates that title molecule is kinetically unstable.

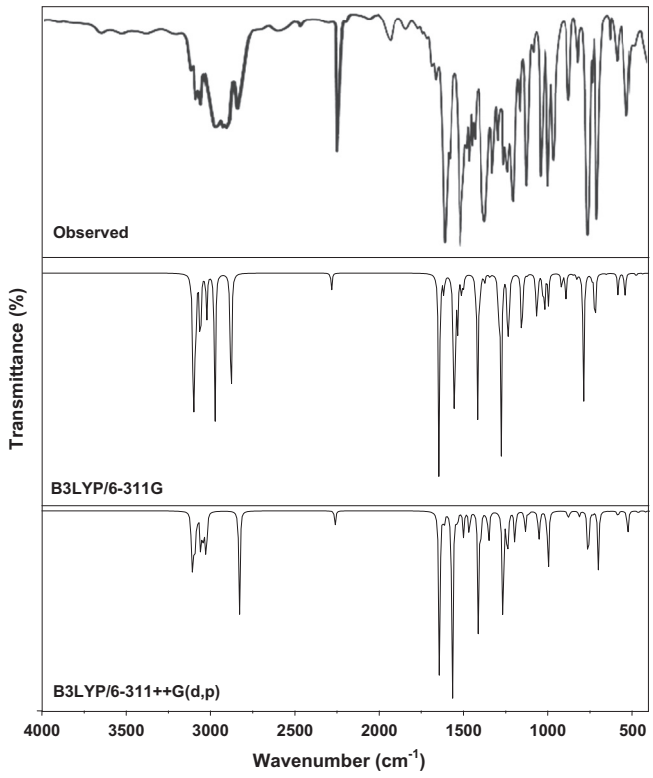

Fig. 2. Experimental and calculated FT-IR spectrum of N-(2-cyanoethyl)-N-methylaniline.

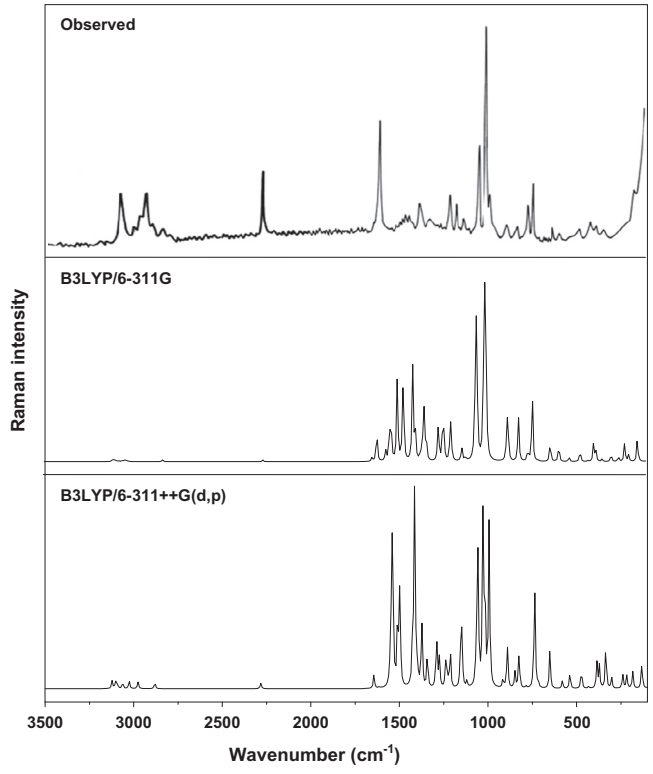

Fig. 3. Experimental and calculated FT-Raman spectrum of N-(2-cyanoethyl)-N-methylaniline.

TD-DFT/B3LYP/6-311++G(d,p) calculated 3D HOMO and LUMO plots of title molecule are displayed in Fig. 4. As can be seen from Fig. 4, the HOMO is localized over the C1—C2, C1—C6, C3—C4, and C4—C5 of molecule. The LUMO localized on the substitution on the ring. It can be said that repulsive interaction between H atom of ring and H atom of methyl in substitution gives rise to twist of substitution. Attractive interaction due to the methylene and cyano groups bonding – like interaction forces the ring to stay in the plane of title molecule and does not allow twisting. DFT/B3LYP/6-311++G(d,p) method produces almost the same HOMO and LUMO plots of title molecule in vacuum.

Molecular electrostatic potential

In the present study, the MEP is a useful property to study reactivity given that an approaching electrophile will be attracted to negative regions (where the electron distribution effect is dominant). In the majority of the MEPs, while the maximum negative region which preferred site for electrophilic attack indicates as red color, the maximum positive region which is the preferred site for nucleophilic attack symptoms as blue color. The importance of MESP lies in the fact that it simultaneously displays molecular size, shape as well as positive, negative and neutral electrostic potential regions in terms of color[1] grading (Fig. 5) and is very useful in research of molecular structure with its physiochemical property relationship [34–36]. The resulting surface simultaneously displays molecular size and shape and electrostatic potential value.

The MEP map in case of N-(2-cyanoethyl)-N-methylaniline suggests that the potential swings widely between hydrogen atoms of ring, methylene, and methyl groups (blue). The nitrogen (≡N) atom reflect the most electronegative region and have excess negative charge, and the hydrogen atoms attached to the ethyl and methylaniline group beat the brunt o positive charge (blue region). The carbon atoms of ring shows green region.

The different values of the electrostatic potential at the surface are represented by different colors. Potential increases in the order red < orange < yellow < green < blue. The color code of these maps is in the range between −0.1 a.u. (deepest red) to 0.1 (deepest blue) an title compound, where blue indicates the strongest attraction and red indicates the strongest repulsion. Regions of negative V(r) are usually associated with the lone pair of electronegative atoms. As can be seen from the MEP map of the title molecule, while regions having the negative potential are over the electronegative atom (≡N atom), the regions having the positive potential are over the hydrogen atoms. If compared, the maximum negative potential values are −0.813 a.u. The electrostatic charges for the color comparison are shown in Fig. 5.

UV–Vis spectra analysis

Ultraviolet spectrum of CMA is shown in Fig. 6. Absorption maximum (λ_{max}) of the molecule has investigated by various theoretical results [37] and it is calculated by TD-DFT (B3LYP) method. The calculated visible absorption maximum of λ which is a function of the electron availability has been reported in Table 5. On the basis of fully optimized ground-state structure, TD-DFT calculations have been used to determine the low-lying excited states of CMA. The calculated results involving the vertical excitation energies, oscillator strength (f) and wavelength are carried out. According to Frank–Condon principle, the maximum absorption peaks (λ_{max}) correspond in a UV–visible spectrum to vertical excitation. The electronic transition predicted by TD-DFT/B3LYP/6-311++G(d,p) method as shown in Fig. 6. The prominent transition in CMA is n → π* as the compound has nitrogen as lone pair along

[1] For interpretation of color in Fig. 5, the reader is referred to the web version of this article.

Table 3
Second-order perturbation theory analysis of Fock matrix in NBO basis corresponding to the intramolecular bonds of N-(2-cyanoethyl)-N-methylaniline.

Donor (*i*)	ED (*i*) (e)	Acceptor (*j*)	ED (*j*) (e)	[a]*E*(2) (kJ mol^{-1})	[b]*E*(*j*) − *E*(*i*) (a.u.)	[c]*F*(*i*,*j*) (a.u.)
Within unit 1						
σC1—C2	1.97341	σ*C1—C6	0.02145	4.14	1.28	0.065
		σ*C1—N7	0.03654	0.80	1.07	0.026
		σ*C2—C3	0.01503	3.21	1.29	0.058
σC2—H8	1.97561	σ*C3—C4	0.01593	3.38	1.11	0.028
σC3—H9	1.98039	σ*C4—C5	0.01586	3.65	1.11	0.057
σC5—C6	1.97581	σ*C1—N7	0.03654	4.25	1.05	0.06
σN7—C13	1.99157	σ*C1—C2	0.02135	4.59	1.10	0.064
σN7—C17	1.98669	σ*C20—C22	0.02124	1.11	1.06	0.031
σC13—H14	1.98774	σ*N7—C17	0.02068	3.30	0.88	0.048
σC17—H18	1.98129	σ*C1—N7	0.03654	3.22	0.91	0.049
σC17—H19	1.98523	σ*N7—C13	0.01450	3.56	0.87	0.050
σC17—C20	1.97185	σ*C22—N23	0.00912	3.21	1.58	0.064
		π*C22—N23	0.00912	2.45	0.73	0.038
σC20—H21	1.96869	π*C22—N23	0.00912	4.45	0.66	0.048
LP N7	1.78214	π*C1—C6	0.02145	30.29	0.27	0.085
		σ*C13—H14	0.01072	1.84	0.66	0.033
		σ*C13—H15	0.00786	1.80	0.65	0.032
		σ*C13—H16	0.01849	7.17	0.65	0.064
		σ*C17—H18	0.01448	1.99	0.66	0.034
		σ*C17—H19	0.02597	7.57	0.66	0.066
		σ*C17—C20	0.01456	1.84	0.57	0.031
LP N24	1.96918	σ*C20—C23	0.02124	9.81	0.85	0.082

[a] *E*(2) means energy of hyper conjugative interaction (stabilization energy).
[b] Energy difference between donor and acceptor *i* and *j* NBO orbitals.
[c] *F*(*i*,*j*) is the Fock matrix element between *i* and *j* NBO orbitals.

Table 4
The charge distribution calculated by the Mulliken and natural bond orbital (NBO) methods using DFT/B3LYP/6-311++G(d,p) of N-(2-cyanoethyl)-N-methylaniline molecule.

Atoms	DFT/6-311++G(d,p)	
	Atomic charges (Mulliken)	Natural charges (NBO)
C1	0.00253	0.19852
C2	−0.255468	−0.26076
C3	−0.163294	−0.17387
C4	−0.378352	−0.24135
C5	−0.249221	−0.17331
C6	0.291668	−0.26142
N7	0.123763	−0.52075
H8	0.101022	0.20133
H9	0.175061	0.20163
H10	0.137539	0.20119
H11	0.177582	0.20206
H12	0.102765	0.20111
C13	−0.419933	−0.34908
H14	0.129823	0.20215
H15	0.141815	0.18860
H16	0.201641	0.18101
C17	−0.565487	−0.13984
H18	0.144080	0.19946
H19	0.221457	0.18628
C20	0.288643	−0.46353
H21	0.152035	0.23566
C22	−0.280005	0.29308
N23	−0.267324	−0.34270
H24	0.187659	0.23453

with this transition $\pi \rightarrow \pi^*$ transition is also possible. Calculations of molecular orbital geometry show that the visible absorption maximum of this molecule corresponds to the electron transition between frontier orbitals such as translation from HOMO to LUMO. It could be seen that low energy absorption found at 286.13, 295.56, and 295.58 nm belongs to the dipole-allowed π–π^* transition from HOMO to LUMO, in the solvent of water, ethanol, and methanol, respectively. The intense band calculated at 239.15 nm can be attributed to high delocalization of π-electrons in the CMA in water as a solvent. The band calculated at 253.27, 253.22 nm may have slight variation in intensity in both the ethanol and methanol solvents. As can be seen from Table 5, TD-DFT/6-311++G(d,p) method predicts three electronic transitions the calculated absorption wavelength (λ_{max}), excitation energies (E), and force constants values may be slightly shifted by solvent effects. This result was also supported by the analysis of orbital population (see Fig. 6).

First order hyperpolarizabilities

NLO techniques are considered as one among the most structure-sensitive method to study molecular structures and assemblies. Since the potential of organic materials for NLO devices have been proven, NLO properties of many of these compounds have been investigated by both experimental and theoretical methods [7]. The efforts on NLO have been largely devoted to prepare first-order NLO materials using theoretical methods and exploring the structure–property relationships. Quantum chemical calculations have been shown to be useful in the description of the relationship between the electronic structure of the system and it's NLO response. The computational approach allows the determination of the molecular NLO properties as an inexpensive way to design molecules by analyzing their potential before synthesis and to determine the higher order hyperpolarizability tensors of molecule.

The calculated first order hyperpolarizability of title molecule is 0.1602×10^{-30} e.s.u. which is 2 times lower than that of urea. The calculated first order hyperpolarizability (β) values are collected in Table 6. The theoretical calculation seems to be more helpful in the determination of particular components of β tensor than in estabilizing the real values of β. Domination of particular components indicates on a substantial delocalization of charges in those directions. It is noticed that in β_{zzz} direction, the biggest values of hyperpolarizability are noticed and subsequently delocalization of electron cloud is more in that direction. The moderate value of β may be due to π-electron cloud movement from donor to acceptor

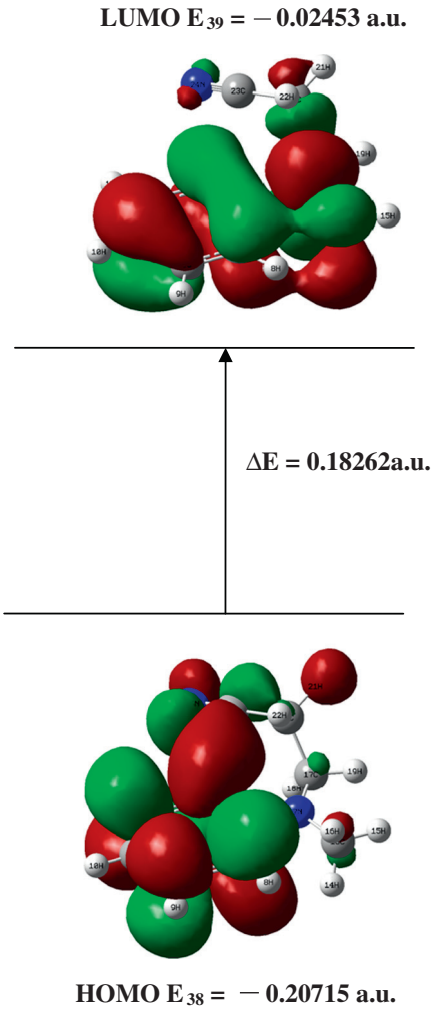

Fig. 4. The atomic orbital composition of the frontier molecular orbital for N-(2-cyanoethyl)-N-methylaniline.

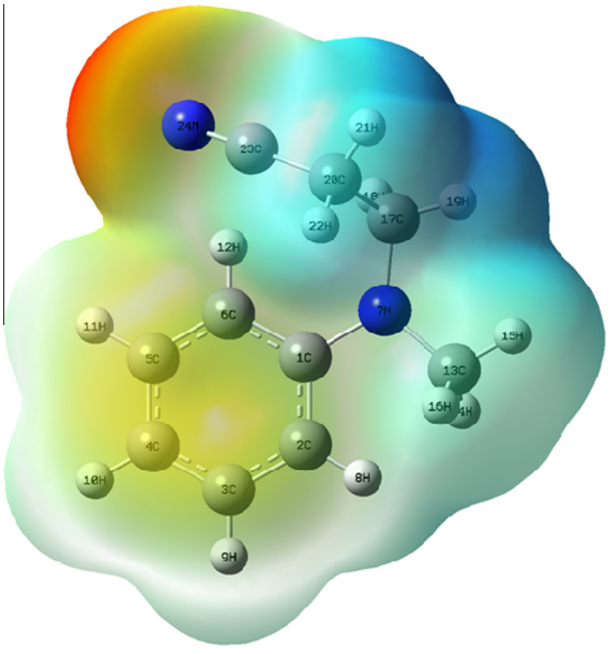

Fig. 5. 3D MESP map of N-(2-cyanoethyl)-N-methylaniline.

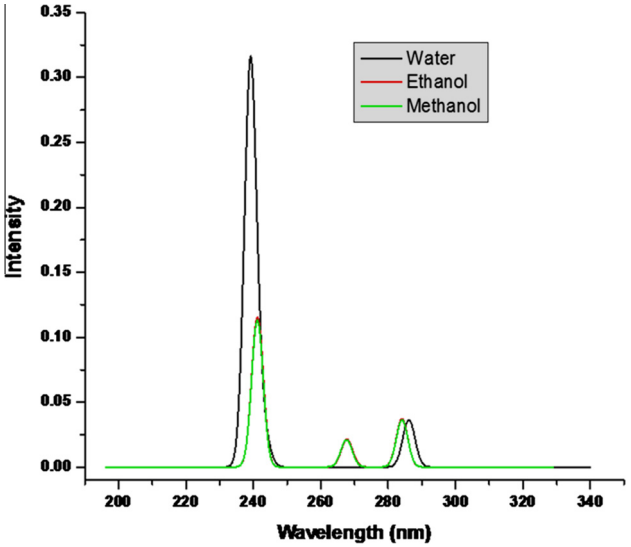

Fig. 6. Calculated UV–Visible spectra for N-(2-cyanoethyl)-N-methylaniline.

which make the molecule polarized and the intramolecular charge transfer possible. The presence of ICT is confirmed with the vibrational spectral analysis.

Thermodynamic properties

Theoretical geometrical parameters represent a good approximation and they are the basis for calculating vibrational frequencies and thermodynamic parameters. The frequency calculations compute the zero point energies, thermal correction to internal energy, Gibb's free energy and entropy as well as the heat capacity for a molecular system. These functions describe the thermodynamic stability of system at given conditions of pressure and temperature. In order to clarify the relations among energetic, structural and reactivity of the title molecule, some of the vibrational and thermodynamic parameters (such as zero point vibrational energy, thermal energy, specific heat capacity, rotational constants, entropy, and dipole moment) of title molecule by DFT/B3LYP/6-311++G(d,p) and DFT/B3LYP/6-311G basis set at 298.15 K and 1 atm pressure are calculated and presented in Table 7. The ZPVE energy is lower in the DFT/B3LYP/6-311++G(d,p) method than by other method. The higher value of ZPVE is 126.50887 kcal mol^{-1} obtained at DFT/B3LYP/6-311G where as smallest one is 125.58049 kcal mol^{-1} obtained at DFT/B3LYP/6-311++G(d,p) method. The total energies found to decreases with higher basis sets. The variation in zero point vibrational energies seems to be insignificant. Likewise, the variation in the total entropy of title molecule at room temperature is only marginal at various methods. The thermodynamic parameters may vary with the temperatures, they are shown in Fig. 7, and the values are reported in Table 8.

The dipole moment of a molecule helps to study the intermolecular interactions involving non-bonded type dipole–dipole interactions, because higher dipole moment, stronger the intermolecular interactions [38]. Direction of the dipole moment vector in a molecule depends on the centers of negative and positive charges. The total thermal energies, vibrational energy contribution to the total energy, rotational constants and dipole moment values are slightly overestimated in DFT/B3LYP/6-311++G(d,p) method. The larger value of dipole moment of title molecule is 3.5679 D obtained at DFT/B3LYP/6-311++G(d,p) whereas the smallest one is 3.4309 D obtained at DFT/B3LYP/6-311G method. The correlation equations

Table 5
Calculated absorption wavelength λ (nm), excitation energies E (eV) and oscillator strengths (f) of N-(2-cyanoethyl)-N-methylaniline.

Water			Ethanol			Methanol			Assignment
λ (nm)	E (eV)	(f)	λ (nm)	E (eV)	(f)	λ (nm)	E (eV)	(f)	
TD-DFT/B3LYP/6-311++G(d,p)									
286.13	4.331	0.0362	295.56	4.1949	0.0371	295.58	4.1947	0.0363	n–π^*
243.06	5.1009	0.0251	279.56	4.4364	0.0213	279.32	4.4388	0.0209	n–π^*
239.15	5.1844	0.3139	253.27	4.8954	0.1153	253.22	4.8963	0.1129	n–π^*

Table 6
The calculated electric dipole moment μ (D) the average polarizability α_{tot} ($\times 10^{-24}$ esu) and the first hyperpolarizability β_{tot} ($\times 10^{-30}$ esu) of N-(2-cyanoethyl)-N-methylaniline using B3LYP/6-311G, and B3LYP/6-311++G(d,p).

Parameters	DFT/6-311G	DFT/6-311++G(d,p)
μ_x	0.1026	2.5293
μ_y	−1.3767	2.1143
μ_z	3.1410	1.3645
μ	3.4309	3.5679
α_{xx}	−71.9453	−96.2616
α_{xy}	3.8373	−7.9468
α_{yy}	−75.2754	−66.9242
α_{xz}	−15.7052	−5.8356
α_{yz}	6.0845	−1.5434
α_{zz}	−95.1033	3.9467
$\langle\alpha\rangle$	−80.7746	−53.0797
α_{tot} (esu)	1.8745×10^{-22}	2.8025×10^{-22}
β_{xxx}	150.4374	176.9824
β_{xxy}	−7.7159	43.1196
β_{xyy}	33.9972	12.2427
β_{yyy}	9.0210	7.0563
β_{xxz}	120.2341	26.0641
β_{xyz}	−17.3876	3.8035
β_{yyz}	55.7520	0.7048
β_{xzz}	149.5388	−13.5241
β_{yzz}	−22.4782	0.7048
β_{zzz}	368.8414	3.2628
β_{tot} (esu)	0.5524×10^{-30}	0.1602×10^{-30}

Table 7
Calculated thermodynamic parameters of N-(2-cyanoethyl)-N-methylaniline employing B3LYP/6-311G, and B3LYP/6-311G++(d,p).

Thermodynamic parameters (298 K)	B3LYP/6-311G	B3LYP/6-311++G(d,p)
SCF energies (a.u.)	−497.723282145	−497.877024213
Total energy (thermal), E_{total} (kcal mol^{-1})	133.601	132.773
Heat capacity at constant volume, Cv (Cal mol^{-1} K)	42.236	42.894
Entropy, S (Cal mol^{-1} K)	106.45	108.295
Total		
Translational	0.889	0.889
Rotational	0.889	0.889
Vibrational	131.824	130.996
Zero point vibrational energy (kcal mol^{-1})	126.50887	125.58049
Rotational constants (GHz)		
A	1.53324	1.42135
B	0.63599	0.6717
C	0.48897	0.57644

between Gibb's free energies, entropies, specific heat capacities with various temperatures are as follows.

$$G^0_{p,m} = 12.18 - 0.037T + 0.00T^2 \times 10^{-4}; \quad (R^2 = 0.996)$$

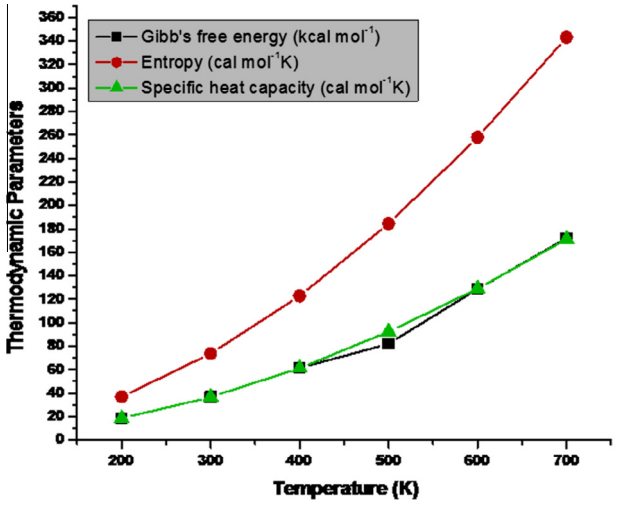

Fig. 7. Calculated thermodynamical parameters of N-(2-cyanoethyl)-N-methylaniline.

Table 8
Thermodynamic properties at different temperatures at the B3LYP/6-311G++(d,p) level for N-(2-cyanoethyl)-N-methylaniline.

T (K)	G^0_p (cal mol^{-1} K^{-1})	S^0_m (cal mol^{-1} K^{-1})	ΔH^0_m (kcal mol^{-1})
200	18.490	36.959	18.501
300	36.849	73.631	36.782
400	61.365	122.773	61.408
500	82.052	184.339	92.286
600	128.898	257.966	129.068
700	171.829	343.138	171.302

$$S^0_m = -0.670 + 0.065T + 0.00T^2 \times 10^{-4}; \quad (R^2 = 1)$$

$$H^0_m = -0.783 + 0.035T + 0.00T^2 \times 10^{-4}; \quad (R^2 = 1)$$

Conclusion

Vibrational spectra of N-(2-cyanoethyl)-N-methylaniline have been recorded and analyzed. Density functional theory method has been used to compute molecular geometry, vibrational wavenumbers, infrared and Raman intensities, NBO and HOMO–LUMO energies. The lowering of the wavenumber is due to the intramolecular charge transfer from the methylaniline group to the ring via π-system. The UV–Vis spectral analysis predicted by TD-DFT/B3LYP/6-311++G(d,p) method show stability of the molecule with the various solvent. The difference in HOMO and LUMO energy supports the charge transfer interaction within the molecule. The first order hyperpolarizability value confirms molecule has moderate NLO property.

References

[1] http://www.chemicalland21.com.
[2] M.J. Frisch, G.W. Trucks, et al., GAUSSIAN 09: Revision A. 02; Gaussian. Inc., Wallingford, CT, 2009.
[3] W.J. Hehre, L. Random, P.V.R. Schleger, J.A. Pople, Ab Initio Molecular Orbital Theory, Wiley, New York, 1986.
[4] N.G. Mirkin, S. Krimm, J. Phys. Chem. 97 (1993) 13887–13895.
[5] V. Arjunan, S. Mohan, Spectrochim. Acta A 72 (2009) 436–444.
[6] D. Zeroka, J.O. Jenson, J. Mol. Struct. (Theochem) 425 (1998) 181–192.
[7] G. Varsanyi, Vibrational Spectra of Benzene Derivatives, Akademiai Kiado, Budapest, 1969.
[8] M. Silverstein, G. Clayton Basseler, C. Morill, Spectrometric Identification of Organic Compounds, Wiley, New York, 1981.
[9] P.D.S. Babuet, S. Periyandi, S. Ramalingam, Spectrochim. Acta A 78 (2011) 1321–1328.
[10] T. Karthick, V. Balachandran, S. Perumal, A. Nataraj, J. Mol. Struct. 1005 (2011) 192–201.
[11] G. Varasanyi, Assignments of Vibrational Spectra of Seven Hundred Benzene Derivatives, Wiley, New York, 1974.
[12] V. Balachandran, A. Nataraj, T. Karthick, J. Mol. Struct. 104 (2013) 114–129.
[13] M. Ramalingam, N. Sundaraganesan, H. Saleem, J. Swaminathan, Spectrochim. Acta A 71 (2008) 23–30.
[14] D. Sajan, J. Binoy, B. Pradeep, K.V. Krishnan, V.B. Kartha, I. Hubert Joe, V.S. Jayakumar, Spectrochim. Acta A 60 (2004) 173–180.
[15] K. Furic, V. Mohack, M. Bonifacic, I. Stefanic, J. Mol. Struct. 267 (1992) 39–44.
[16] K.B. Wiberg, A. Sharke, Spectrochim. Acta A 29 (1973) 583–624.
[17] A. Nataraj, V. Balachandran, T. Karthick, J. Mol. Struct. 1006 (2011) 104–112.
[18] P.J.A. Ribeiro-Claro, L.A.E. Batista de Carvalho, A.M. Amado, J. Raman Spectrosc. 28 (1997) 867–872.
[19] S. Ahmad, P.K. Verma, Ind. J. Phys. B 64 (1990) 50.
[20] D.L. Vein, N.B. Colthup, W.G. Fateley, J.G. Grasselli, The Handbook of Infrared and Raman Characteristic Frequencies of Organic Molecules, Academic Press Inc., San Diego, CA, 1991.
[21] F.R. Dollish, W.G. Fateley, F.F. Bentley, Characteristic Raman Frequencies of Organic Compounds, Wiley, New York, 1974.
[22] L.J. Bellamy, The Infrared Spectra of Complex Molecules, Wiley, New York, 1975.
[23] I. Deady, A.R. Katritzky, R.A. Shanks, R.A. Topsom, Spectrochim. Acta A 29 (1973) 115–121.
[24] T. Saito, M. Yamakawa, M. Takasuka, J. Mol. Spectrosc. 90 (1981) 359–366.
[25] N. Akai, D. Negishi, S. Kudoh, M. Takayanagi, M. Nakata, J. Mol. Struct. 688 (2004) 177–183.
[26] A. Nataraj, V. Balachandran, T. Karthick, J. Mol. Struct. 1038 (2013) 134–144.
[27] S. Ahmad Siddiqui, A. Dwivedi, N. Misra, N. Sundaraganasan, J. Mol. Struct. (Theochem) 827 (2007) 101–106.
[28] C. James, A. Amal Raj, R. Rehunathan, I. Hubert Joe, V.S. Jayakumar, J. Raman Spectrosc. 37 (2006) 1381–1392.
[29] Liu Jun-na, Chen Zhi-rong, Yuan shen-feng, J. Zhejiang University Sci. B 6 (2005) 584.
[30] S. Sebastian, N. Sundaraganesan, Spectrochim. Acta A 75 (2010) 941–952.
[31] X. Assfeld, J.L. Rivail, Chem. Phys. Lett. 263 (1996) 100–106.
[32] G. Gece, Corros. Sci. 50 (2008) 2981–2992.
[33] P.W. Atkins, Physical Chemistry, Oxford University Press, Oxford, 2001.
[34] J.S. Murray, K. Sen, Molecular Electrostatic Potentials, Concepts and 399 Applications, Elsevier, Amsterdam, 1996.
[35] I. Alkorta, J.J. Perez, Int. J. Quantum Chem. 57 (1996) 123–135.
[36] E. Scrocco, J. Tomasi, in: P. Lowdin (Ed.), Advances in Quantum Chemistry, Academic Press, New York, 1978.
[37] M.W. Wong, M.J. Frisch, K.B. Wiberg, J. Am. Chem. Soc. 113 (1991) 4776.
[38] O. Prasad, L. Sinha, N. Kumar, J. Atom. Mol. Sci. 1 (2010) 201–214.